

**A Multi-Grid Control Volume Method
for the Simulation of
Arbitrarily Shaped Slider Air Bearings
With Multiple Recess Levels**

by

Sha Lu and David B. Bogy

Computer Mechanics Laboratory
Department of Mechanical Engineering
University of California
Berkeley, CA 94720

August 1994

Abstract

A new control volume method has been implemented in the CML slider air bearing simulator, which enhances the stability and accuracy of the solution. The scheme for mass flow averaging across clearance discontinuities has been generalized to treat multiple recess depths. The program also contains an adaptive grid option to automatically make better use of the available grid size. Also the implementation of a multi-grid method has reduced the typical solution time by more than an order of magnitude, so the simulator can now be used as an efficient design tool. Furthermore, a graphical user interface integrated with Matlab has been designed and implemented to facilitate the pre and post processing of the simulations. The program has been ported to several UNIX workstations and PCs.

I. Introduction

The Head-Disk Assembly simulator at the Computer Mechanics Laboratory was developed over the past decade. The solution of the generalized lubrication equation is a very important part of the simulator. Miu and Bogy (1986) implemented the factored implicit scheme of White and Nigam (1980). It is a useful and efficient method for dynamic simulations. However, it displays numerical instability for high bearing numbers. Cha (1993) improved the stability by partially incorporating Patankar's (1980)

Power-Law scheme, but a somewhat complicated linearization was used in his formulation. Furthermore, time marching was employed for the steady state solution, which reduces the computational efficiency.

Patankar (1980) presented a simple, unified control volume formulation for a general class of convection-diffusion differential equations. The Power-Law scheme that he proposed for the convective term solved the stability problem normally associated with the central difference scheme. The generalized lubrication equation falls into the category of these convection-diffusion equations. Therefore, Patankar's control volume method has been implemented in the CML air bearing simulator. Due to the remarkable stability of this scheme, the pseudo-transient term can be omitted in the equation for the steady state solution. Consequently, the steady state solution is achieved by direct iteration, eliminating the complication of time stepping.

The nonlinearity of the equation is dealt with iteratively. At each iteration, the result of discretization is approximated by a linear system, which is also solved through iteration. Fast convergence depends on the use of an efficient iteration method. With single grid iterative methods rapid progress toward convergence can be obtained only during the first few iterations. Brandt (1977) demonstrated that only those error components with wavelengths comparable to the mesh size are smoothed efficiently, and that error components with longer wavelengths are smoothed at progressively slower rates.

The multi-grid technique, originally developed for the efficient solution of linear elliptic partial differential equations (Brandt, 1977), has recently gained popularity, especially in the field of computational fluid dynamics and heat transfer. In the field of

lubrication, the multi-grid method has been used to solve EHD lubrication problems (Lubrecht, 1987 and Osborn et al, 1992). The multi-grid method recognizes the fact that the long wavelength (smooth) error components on a fine grid are shorter relative to the mesh size when seen from a coarser grid. Thus, they can be smoothed more efficiently if the solution is moved to a coarser grid. By moving the solution back and forth between a set of different grid levels, both long and short wave length error components can be smoothed efficiently.

A multi-grid method based on the one proposed by Shyy and Sun (1992) has been implemented in the CML air bearing simulator. The full approximation storage used in this formulation deals more efficiently with the nonlinearity of the equation than the simpler correction storage. The efficiency of the multi-grid method is optimum compared to single grid iterative methods in the sense that the computation effort is linearly proportional to the number of degrees of freedom. The multi-grid method becomes even more superior when the degrees of freedom become larger.

The realization of the multi-grid method makes the current formulation competitive in efficiency with the factored implicit scheme, even for dynamic simulations, and it does not have the numerical instability for high bearing numbers that is inherent in the latter.

Cha (1993) implemented the technique introduced by Kogure et. al. (1983) to deal with the clearance discontinuity. It averages the mass flow across the discontinuity by weighting the mass flow contributions from both sides of the discontinuity. That implementation allows only one recess depth, but slider designs are becoming more complicated in order to achieve low and uniform fly height across the disk, so one recess depth may no longer be sufficient. The mass flow averaging scheme has now been

generalized to allow different recess depths for different regions . In this implementation, instead of checking where the discontinuity is located on the control volume boundary, we average the mass flows at many points along the boundaries to account for the discontinuity, if any.

An adaptive grid method based on the pressure gradient field has also been implemented. After obtaining the pressure distribution using the initial grid, we calculate the pressure gradient field. The grid is then redistributed so that the grid is concentrated in regions where the pressure gradient is high. Thus, more accurate results can be obtained using a given grid size.

During the slider design process rail shapes need to be modified frequently to achieve the design goals. Inputting the rail shapes graphically by use of a mouse not only makes modification easier, it can also help avoid errors. To facilitate the pre and post processing of the simulation, and to provide a convenient way of specifying parameters as well as checking the results, we developed a graphical interface using Matlab software.

II. Discretization of the Generalized Lubrication Equation

The governing equation in the classical hydrodynamic lubrication theory is called the Reynolds equation. Due to the small spacing (high Knudsen numbers) in the slider air bearings, the continuum and no-slip assumptions in the classical theory are violated. Several modifications to account for the rarefaction effects have been proposed (Burgdorfer, 1959, Hsia and Domoto, 1983, Gans, 1985 and Fukui and Kaneko, 1988).

These generalized forms of the classical lubrication equation can be written as (Ruiz, 1989),

$$\sigma \frac{\partial PH}{\partial T} = \frac{\partial}{\partial X} (QPH^3 \frac{\partial P}{\partial X} - \Lambda_x PH) + \frac{\partial}{\partial Y} (QPH^3 \frac{\partial P}{\partial Y} - \Lambda_y PH), \quad (2.1)$$

where $P = p / p_a$, $H = h / h_m$, $T = \omega t$, $X = x / L$, $Y = y / L$ are the non-dimensionalized pressure, bearing clearance, time, coordinate in slider length direction and coordinate in slider width direction, respectively; p_a is the atmospheric pressure; h_m is the reference clearance at the trailing edge center; ω is the angular velocity of the disk; L is the length of the slider; $\Lambda_x = \frac{6\mu UL}{P_a h_m^2}$ and $\Lambda_y = \frac{6\mu VL}{P_a h_m^2}$ are the bearing numbers in the x and y directions, respectively; U and V are the x and y velocity components, respectively; $\sigma = \frac{12\mu\omega L^2}{P h_m^2}$ is the squeeze number; Q is the flow factor, and assumes different forms

depending on the type of correction model used,

$Q = 1,$	Continuum Model
$Q = 1 + 6a \frac{K_n}{PH},$	First Order Slip Model
$Q = 1 + 6 \frac{K_n}{PH} + 6(\frac{K_n}{PH})^2,$	Second Order Slip Model
$Q = f(\frac{K_n}{PH}),$	Fukui-Kaneko Model

where $a = \frac{2-\alpha}{\alpha}$ and a is the accommodation factor; K_n is the Knudsen number; $f(\frac{K_n}{PH})$

is as given by Fukui and Kaneko (1988).

In the earlier discretizations of the lubrication equation in the CML simulator (Miu and Bogoy, 1986 and Cha, 1993), linearization was used, and the resulting discretized equation was unnecessarily involved. Patankar (1980) described a unified

control volume formulation for a general class of convection-diffusion equations having the following form:

$$\frac{\partial}{\partial t}(\rho\phi) + \text{div}(\rho\mathbf{u}\phi) = \text{div}(\Gamma\text{grad}\phi) + S, \quad (2.2)$$

where ϕ is the dependent variable, Γ is the diffusion coefficient, \mathbf{u} is the flow velocity and S is the source term.

The dimensional form of Eq.(2.2) can be written as

$$\frac{\partial}{\partial t}(\rho\phi) + \frac{\partial J_x}{\partial x} + \frac{\partial J_y}{\partial y} = S, \quad (2.3)$$

where J_x and J_y are the total (convection plus diffusion) fluxes defined by

$$J_x \equiv \rho u\phi - \Gamma \frac{\partial \phi}{\partial x}, \quad (2.4a)$$

$$J_y \equiv \rho v\phi - \Gamma \frac{\partial \phi}{\partial y}, \quad (2.4b)$$

where u and v denote the x and y components of \mathbf{u} .

It is clear that Eq.(2.1) is a special case of Eq.(2.3-2.4), with $\phi = \mathbf{P}$, $\rho = \mathbf{H}$, $u = \mathbf{A} / \sigma$, $v = \mathbf{A} / \sigma$, and $\Gamma = QPH^3 / \sigma$. Here, the diffusion coefficient Γ is not a constant.

Next, the discretization of Eq.(2.3) using Patankar's (1980) control volume method will be described briefly, using an implicit method for the unsteady term . Other methods of time discretization (for example, the Crank-Nicolson scheme) can be dealt with similarly. In the case of the steady state solution, the time derivative term can be

omitted completely in this formulation. The integration of (2.3) over the control volume shown in Figure 2.1 gives,

$$\frac{(\rho_p \phi_P - \rho_p^0 \phi_p^0) \Delta x \Delta y}{\Delta t} + J_e - J_w + J_n - J_s = (S_c + S_p \phi_p) \Delta x \Delta y, \quad (2.5)$$

where the superscripts denote the quantities at the last time step; the source term S has been decomposed into a linearized function of ϕ_p with coefficients S_c and S_p ; J_e, J_w , etc. are the integrated total fluxes over the control-volume faces.

The evaluation of the total fluxes, which need to be approximated using the values of the dependent variable at neighboring points, can cause difficulty in the numerical solution. It seems natural to use the central difference scheme, for example,

$$\begin{aligned} \mathbf{J}_e &\equiv (\rho u \phi)_e - (\mathbf{I} + \mathbf{ax})_e \\ &= \frac{1}{2} (\rho u)_e (\phi_E + \phi_P) - \Gamma_e \frac{(\phi_E - \phi_P)}{(\delta x)_e}, \end{aligned} \quad (2.6)$$

etc., to represent the total fluxes. Eq.(2.5) can then be regrouped into the form

$$a_P \phi_P = a_E \phi_E + a_W \phi_W + a_N \phi_N + a_S \phi_S + b. \quad (2.7)$$

However, using the obvious central difference scheme to represent the convective part often leads to instability, because the coefficients in Eq. (2.7) may become negative. Different schemes have been proposed to overcome this difficulty. The corresponding coefficients of Eq. (2.7) can be summarized in the following unified form, after Patankar (1980),

$$a_E = D_e A(|P_e|) + \max(-F_e, 0), \quad (2.8a)$$

$$a_W = D_w A(|P_w|) + \max(F_w, 0), \quad (2.8b)$$

$$a_N = D_n A(|P_n|) + \max(-F_n, 0), \quad (2.8c)$$

$$a_S = D_s A(|P_s|) + \max(F_s, 0), \quad (2.8d)$$

$$b = S_C \Delta x \Delta y + \frac{\rho_P^0 \Delta x \Delta y \phi_P^0}{\Delta t}, \quad (2.8e)$$

$$a_P = a_E + a_W + a_N + a_S + (F_e - F_w + F_n - F_s) + \frac{\rho_P \Delta x \Delta y}{\Delta t} - S_P \Delta x \Delta y, \quad (2.8f)$$

where $F \equiv \rho u$, $D \equiv \frac{\Gamma}{\delta x}$, $P = \frac{\rho u \delta x}{\Gamma}$ (at e and w faces), or $F \equiv \rho v$, $D \equiv \frac{\Gamma}{\delta y}$, $P = \frac{\rho v \delta y}{\Gamma}$ (at n and s faces) are the convection coefficient, diffusion coefficient and cell Peclet number, respectively; the function $A(|P|)$ depends on the convective scheme chosen,

$1 - 0.5 P $,	Central difference
1 ,	Upwind
$\max(0, 1 - 0.5 P)$,	Hybrid
$\max(0, (1 - 0.1 P)^5)$,	Power-law
$ P / [\exp(P) - 1]$.	Exponential

The exponential scheme is rarely used because exponentials are expensive to compute and it is based on the exact solution only for steady one dimensional linear problems without the source term, therefore it is not necessarily accurate for more general problems.

The QUICK scheme originally devised by Leonard (1979) employs a three-point upstream-weighted quadratic interpolation method to evaluate the dependent variable at the control volume faces, therefore it has a higher order of accuracy than the central

difference scheme. Hayase et. al. (1992) proposed a formulation of QUICK through rearrangement of the source term, which has better convergence performance than other QUICK schemes. They also cast the central difference scheme in the upwind form to achieve better stability. The QUICK scheme of Hayase et. al. (1992) has been implemented in the current simulator, along with the central difference scheme in hybrid form. The Upwind, Hybrid and Power-law schemes are also implemented and available to be selected by the user.

It is found that the current central difference scheme converges for some simple straight bearing designs. But it displays some false peaks at the trailing edge when a coarse grid is used. The convergence rate is slower than that for other schemes and divergence occurs for complicated designs. Therefore, the central difference scheme is not suitable for actual simulations.

The QUICK scheme is basically stable in the sense that it has little difficulty in converging. But it also displays slight false peaks at high bearing numbers. The amount of computation is also higher than that for other schemes.

The Upwind scheme is the least accurate among all schemes for well converged solutions (no instability). It consistently yields lower pressure peaks and total bearing forces.

The Hybrid scheme and Power-law scheme have similar orders of accuracy and both possess good convergence characteristics. They should be used in the practical air bearing simulations.

The system (2.7) is solved using the alternating direction line sweep method (Patankar, 1980) combined with the multi-grid method described in section IV.

III. Mass Flow Averaging Scheme

Cha (1993) implemented the mass flow averaging scheme of Kogure et al. (1983) to deal with clearance discontinuity. In this technique the mass flow rate (flux) on a control volume boundary with discontinuity is averaged by appropriately weighting the contribution from both sides of the discontinuity. However, only one level of recess depth is considered in Cha's implementation. In order to achieve better flying characteristics, slider designs are becoming more complicated, and designs with multiple recess levels have also emerged, calling for a more general implementation of the mass flow averaging scheme.

In Cha (1993), the location of the discontinuity on the control volume boundary is determined analytically by calculating the intersection of the rail boundary and the control volume boundary, thus the weights for mass flow on both sides of the discontinuity are obtained. However, this method is difficult to use in the general case of multiple recess levels. Therefore, an alternative method has been used in the current implementation (Figure 3.1). It is assumed that no more than one discontinuity is present on each side of the control volume boundary (the grid is fine enough), since it is not practical to resolve multiple discontinuities on one side of the control volume. First, the recess depths at many points are sampled on the control volume boundary. Then the maximum h_{\max} , minimum h_{\min} , and the average h_{avg} are obtained. Next, by assuming the recess at any point along the boundary is either h_{\max} or h_{\min} , and knowing h_{avg} , the proportion of the

length L_1 and L_2 on each side of the discontinuity can be approximated. Currently, 20 points are used on each side. This simple method can be used for general multiple recess cases.

IV. Multi Grid Method

In order to obtain the air bearing pressure with a certain degree of accuracy, a large number of grid points is usually required. With so many degrees of freedom, a tremendous amount of memory is required if a direct method is used. Therefore, an iterative method is the only practical solution. It is well known that with a conventional iterative method, the solution converges rapidly during the first few iterations, then the convergence rate becomes progressively slower. This is because conventional methods are only efficient in smoothing those error components with wavelengths comparable to the mesh size, and the error components with longer wavelengths are smoothed at progressively slower rates (Brandt, 1977). The multi-grid method recognizes the fact that the long wavelength error components are relatively shorter when seen from a coarser grid. By moving the solution back and forth among a set of coarse to fine grids, both the long wavelength and short wavelength error components are smoothed effectively.

The current implementation is based on the FMG-FAS (full multi grid-full approximation storage) method used by Shyy and Sun (1992), which was designed to deal with nonlinear problems more effectively than the simpler CS (correction storage) scheme.

The computation is carried out on a series of grids, G_k , with the corresponding solution $\langle \psi_k \rangle$, where $k=1,2,3,4,5$ in the current implementation. G_5 is the finest mesh, and the mesh reduces by a factor of two when the level is lowered by one. The converged solution satisfies the matrix representation of Eq.(2.7):

$$[\alpha_k] \langle \psi_k \rangle = \langle \zeta_k \rangle, \quad (4.1)$$

where the coefficient matrix $[a_k]$ and the source vector $\langle \zeta_k \rangle$ are based on the final solutions of $\langle \psi_k \rangle$, but they are estimated using the intermediate solution before convergence. The full approximation storage scheme described by Shyy and Sun is briefly given below.

The procedure of the multi-grid cycling is illustrated in Figure 4.1, after Shyy and Sun (1992), with slight difference in the number of iterations at each level. In a V cycle at each grid level, the solver performs a few iterations on the fine grid, then the residual is restricted (interpolated) to the next coarser grid to form the equation on that grid. A few iterations are then performed on that grid. The same procedure goes on to the coarsest grid. After a fixed number of iterations on the coarsest grid, the solution increment is prolonged (interpolated) back to the next finer grid. A small number of iterations is performed and then the solution is again prolonged to the next finer grid until the finest grid on that level is reached. This completes the V-cycle. The numbers of iterations indicated in Figure 4.1 are the upper limits. Fewer iterations may actually be performed if convergence is reached.

A good initial approximation may reduce the number of iterations required to reach convergence. To get a better initial guess, it is helpful to interpolate the solution on a coarse grid to the fine grid. In the full multi grid strategy, the solution is first obtained

on the coarsest level and then interpolated to the next grid. The V-cycle is performed on that level until convergence is obtained. Then the solution is interpolated to the next finer grid and the V-cycle is again performed. The final solution is obtained when the V-cycle converges on the finest grid.

It has been observed that a savings of more than one order of magnitude in computation time can be achieved with the typical grid size used in air bearing simulations, The multi-grid method becomes even more superior when a larger grid size is used.

V. Adaptive Grid

The finite difference grid needs to be generated before the solution process starts. A uniform grid is usually not a good one because, while it could be insufficient in high pressure gradient areas, it could also be wasteful in near constant pressure regions. One commonly used method to adjust grid distribution is the piecewise geometric progression method, where the ratio of successive grid increments remains constant in each segment. This method was used in the previous version of the simulator, but with little flexibility. In the current implementation, the grid generation has been generalized to allow arbitrary piecewise geometric progression.

It is not very convenient to prescribe a grid distribution using the above method for every case, and it is sometimes difficult to arrive at a satisfactory distribution. Therefore, some kind of automatic mesh generation scheme is desirable. To this end, an adaptive grid method has been implemented. While it does not guarantee the 'best' grid for all rail designs, it does provide very reasonable grid distribution in most cases. In this method, the pressure gradient field is first obtained from the initial calculation, which usually starts from a uniform grid. Then, the grid is redistributed using the pressure gradient field as the grid density function and the pressure solution is obtained again. This is normally done twice in the program.

Some user control is available. For any location in the x direction, there are many different y stations, and vice versa. Either the averaged pressure gradient ($ipmax=0$) or the maximum pressure gradient ($ipmax=1$) among these different stations can be used as the grid density at that location. The calculated pressure gradient may not be used directly as a grid density function. One issue is that the pressure gradient may be close to zero in certain regions, whereas some minimum grid density is needed to reduce the error in the integrated bearing load. Therefore one parameter called *difmax*, which is the allowable ratio of maximum to minimum pressure gradient, is used in the program. For any pressure gradient below that level, it is assigned the minimum grid number. Another issue is that the calculated pressure gradient may vary abruptly from one location to the next, whereas a smoother grid density is desired to reduce the discretization error induced by grid change. To this end, some smoothing technique is employed in the program so that the pressure gradient at one location affects not only the grid density at that location, but it also has an exponentially decaying effect on the neighboring locations. The parameter *decayfactor* controls how fast its influence on the neighboring locations decays. For large *decayfactor*, the decay is fast so that there is less smoothing effect.

In most slider air bearing designs, there is a taper region at the leading edge. This is perhaps the most important area to resolve in a simulation in order to obtain an accurate bearing load. There is usually a rapid rise in pressure near the taper end. When the grid resolution is not enough there, the pressure either does not rise high enough or overshoots to false peaks so that the entire pressure level is shifted and the total bearing load is grossly wrong. When the grid is prescribed manually using the piecewise geometric progression method, it is of course possible to concentrate grid sufficiently at the taper. However, when the adaptive grid is used, sometimes the grid concentration there may not be enough if only the calculated grid density is used. Therefore, an automatic concentration algorithm is used at the taper end. The program checks the number of grid points covered in the pressure rise region near the taper end. The grid is artificially concentrated until it meets the preset density level.

Figure 5.1 illustrates the rail design of the IBM tri-rail slider. The 3-D pressure distribution obtained for this slider is shown in Figure 5.2. It can be observed that the pressure profile is smooth and all areas are covered by sufficient grid points. The final grid distribution is shown in Figure 5.3. The grid density is high in the rail areas, particularly near the taper end and the rail trailing edges, where the pressure gradient is high.

VI. User Interface

During the ABS design process, rail shapes need to be modified constantly to achieve the design goal and many simulation runs may need to be completed. It is very important to have an easy way of entering and modifying rail designs and other defining parameters, as well as checking the results. To this end, a graphical interface using the Matlab software has been implemented. Matlab provides an environment for doing mathematical manipulations. It has powerful graphics functions and a way to implement customized graphical interfaces. Within the interface, parameters defining the problem can be entered through a menu, the rail shapes can be entered and modified graphically using the mouse, and graphics functions are also available for post processing. The interface is described in more detail by Lu and Bogy (1994).

VII. Summary

Significant improvements have been made in the CML air bearing simulator.

- Due to the implementation of a multi-grid method, the solver efficiency is dramatically increased. The simulator has become a powerful design tool. It is now possible to run many simulations in a relatively short time, thus enabling the exploration of many different parameters in the design process without resorting to costly and time consuming prototyping.

- The current implementation of the mass flow averaging scheme allows different recess levels, making the simulator more versatile.
- The adaptive grid generation and the graphical interface makes the program very easy to use.

Acknowledgment

This research project is supported by the Computer Mechanics Laboratory, at the University of California at Berkeley.

References

Burgdorfer, A., 1959, "The Influence of the Molecular Mean Free Path on the Performance of Hydrodynamic Gas Lubricated Bearings," *ASME Journal of Basic Engineering*, Vol.81, pp.94-100.

Brandt, A., 1977, "Multi-level adaptive solutions to boundary-value problems", *Mathematics of Computation*, Vol. 3 1, p.333.

Cha, E.T., 1993, "Numerical Analysis of Head-Disk Assembly Dynamics for Shaped Rail Sliders with Sub-ambient Pressure Regions", *Doctoral Dissertation*, Dept. of Mech. Eng., UC Berkeley.

Fukui, S. and Kaneko, R., 1988, "Analysis of Ultra-Thin Gas Film Lubrication Based on Linearized Boltzmann Equation: First Report — Derivation of a Generalized Lubrication

Equation Including Thermal Creep Flow,” *ASME Journal of Tribology*, Vol. 110, pp.335-341.

Gans, R., 1985, “Lubrication Theory at Arbitrary Knudsen Number,” *ASME Journal of Tribology*, Vol. 107, pp. 431-433.

Hayase, T., Humphrey, J.A.C. and Greif, R., 1992, “A Consistently Formulated QUICK Scheme for Fast and Stable Convergence Using Finite-Volume Iterative Calculation Procedures”, *Journal of Computational Physics*, Vol. 98, pp. 108-118.

Hsia, Y.T. and Domoto, G.A., 1983, “An Experimental Investigation of Molecular Rarefaction Effects in Gas Lubricated Bearings at Ultra-Low Clearances,” *ASME Journal of Lubrication Technology*, Vol. 105, pp. 120-130.

Kogure, K., Fukui, S., Mitsuya, Y. and Kaneko, R., 1983, “Design of Negative Pressure Slider for Magnetic Recording Disks”, *Journal of Lubrication Technology*, Vol. 105, pp. 496-502.

Leonard, B. P., 1979, “A Stable and Accurate Convection Modeling Procedure Based on Quadratic Upstream Interpolation”, *Computer Methods in Applied Mechanics and Engineering*, Vol. 19, pp. 59-98.

Lu, S. and Bogy, D.B., 1994, “CML Air Bearing Simulator User’s Manual”, *CML Report* (to appear), Dept. of Mech. Eng., UC Berkeley.

Miu, D.K. and Bogy, D.B., 1986, "Dynamics of Gas-lubricated Slider Bearings in Magnetic Recording Files — Part II: Numerical Simulation", *ASME Journal of Tribology*, Vol. 108, October, pp.589-593.

Patankar, S.V., 1980, *Numerical Heat Transfer and Fluid Flow*, McGraw-Hill, New York.

Ruiz, O.J., 1989, "Numerical Simulation of the Head-Disk Assembly Dynamics in Magnetic Recording Disk Files", *Doctoral Dissertation*, Dept. of Mech. Eng., UC Berkeley.

Shyy, W. and Sun, C.S., 1993, "Development of a Pressure-correction/Staggered-grid Based Multi grid Solver for Incompressible Recirculating Flows", *Computers and Fluids*, Vol.22, No. 1, pp.5 1-76.

White, J.W. and Nigam, A., 1980, "A Factored Implicit Scheme for the Numerical Solution of the Reynolds Equation at Very Low Spacing", *ASME Journal of Lubrication Technology*, Vol. 105, pp.485-490.

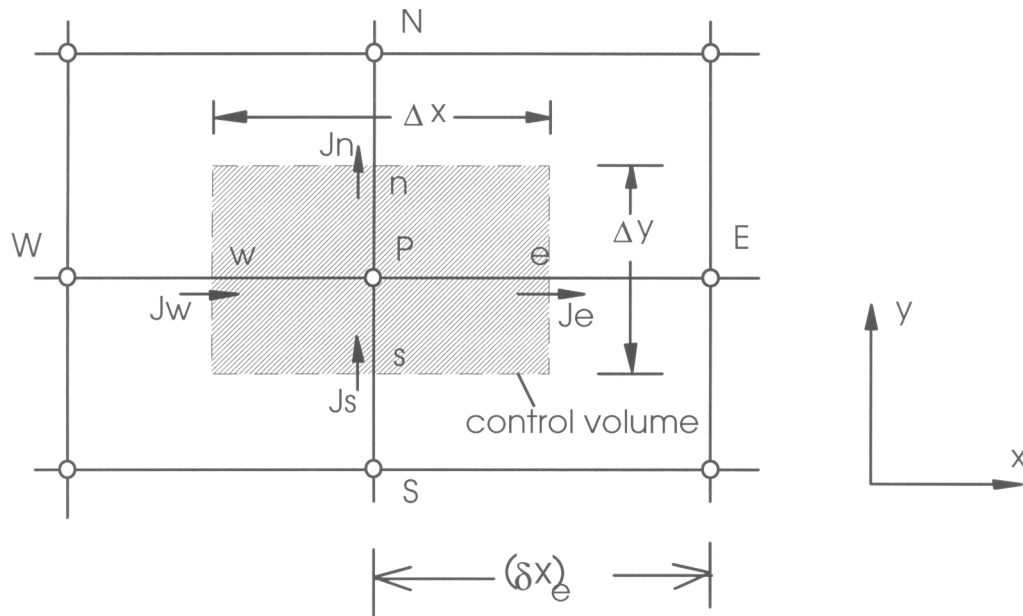


Figure 2.1. Illustration of the control volume (after Patankar, 1980)

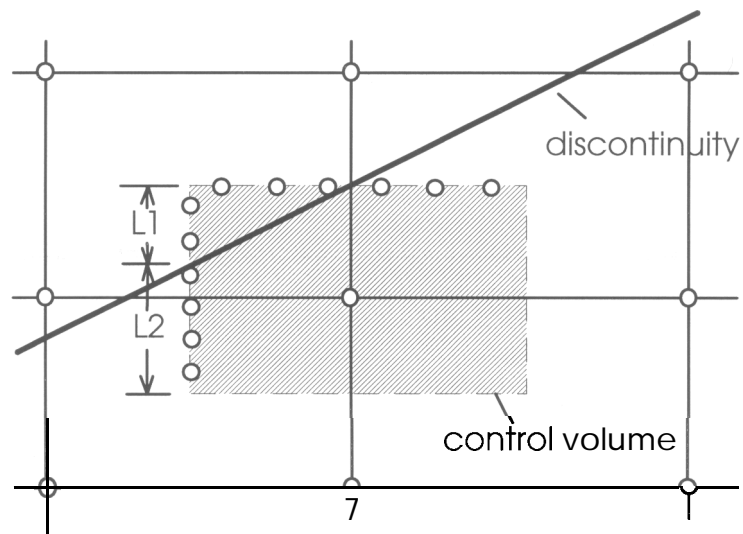


Figure 3.1. Mass flow averaging scheme for clearance discontinuity

Full Multigrid (FMG) V-cycle

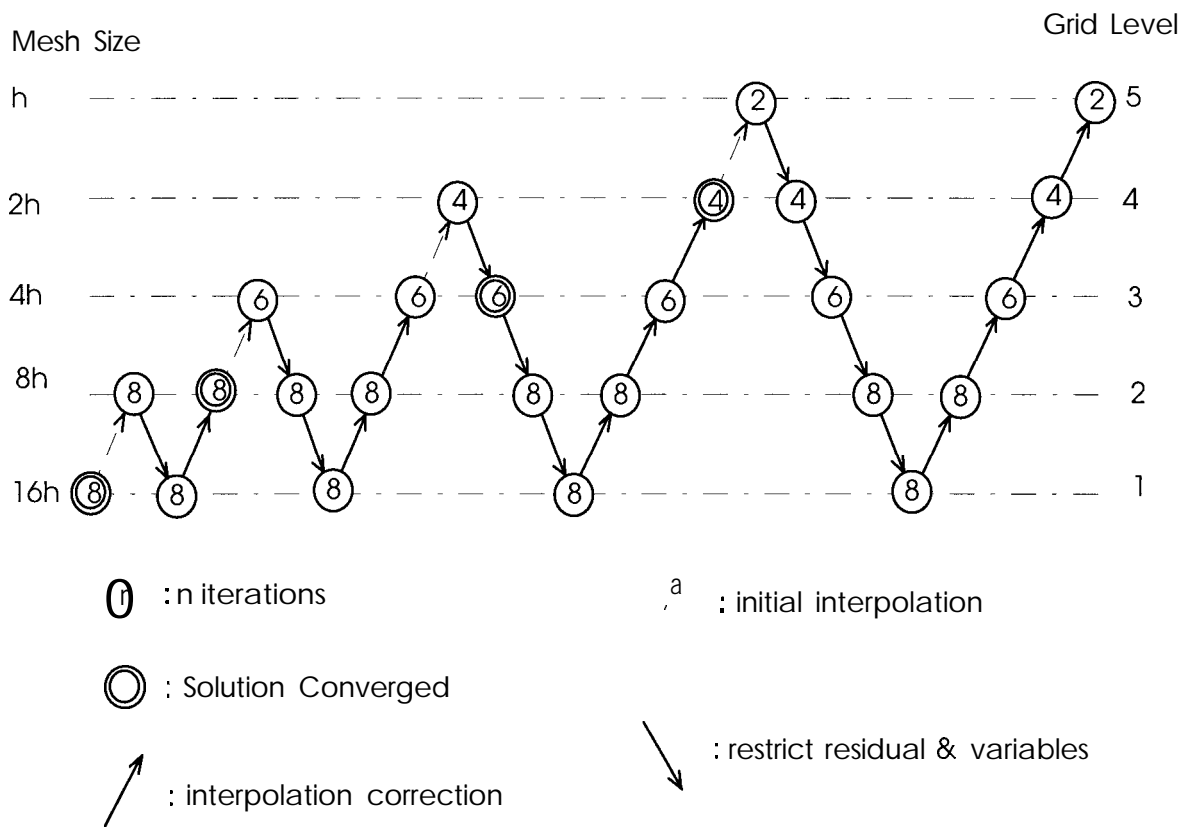


Figure 4.1. The full multi grid procedure (after Shyy and Sun, 1992)

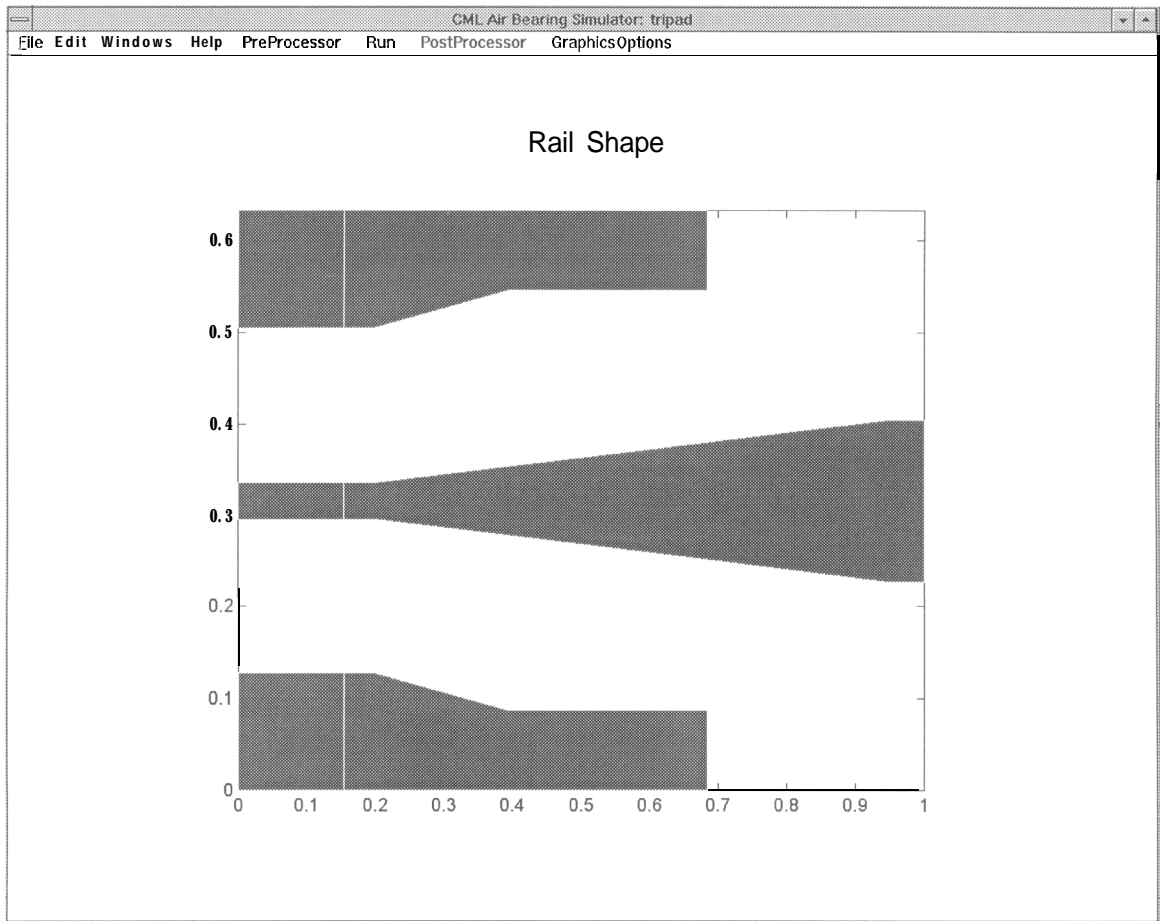


Figure 5.1 IBM Tri-rail Slider

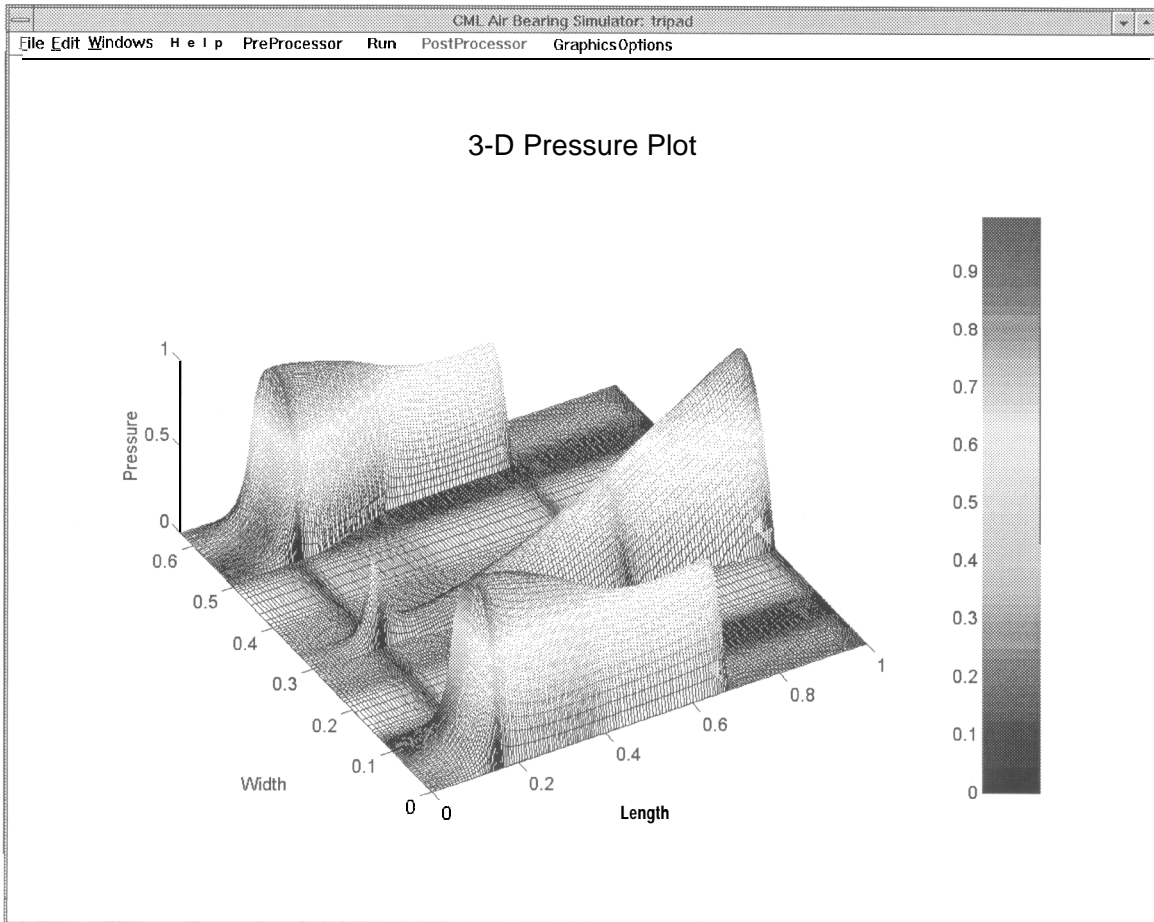


Figure 5.2 Pressure distribution for the Tri-rail slider

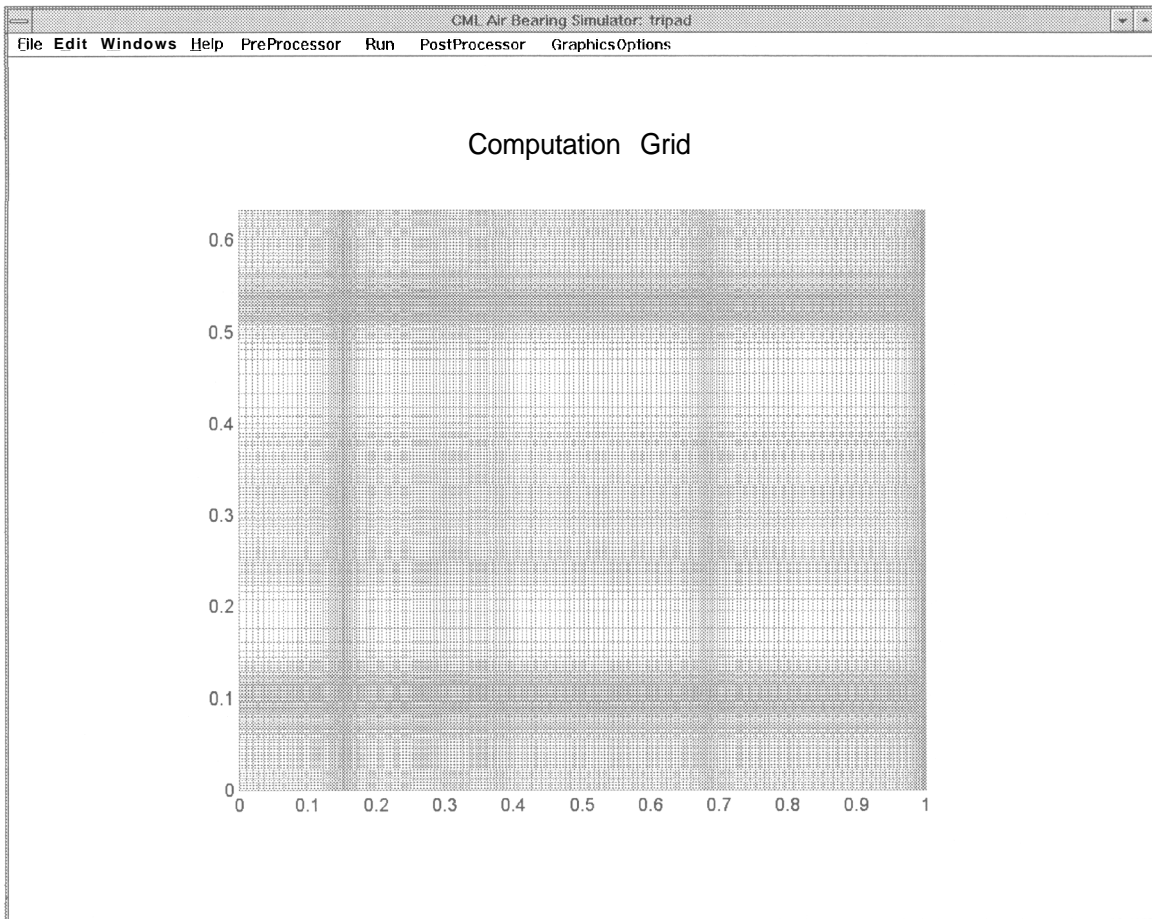


Figure 5.3 Final computation grid for Tri-rail slider